12-2021

Enzyme kinetics, molecular docking, and in silico characterization of canary seed (Phalaris canariensis L.) peptides with ACE and pancreatic lipase inhibitory activity
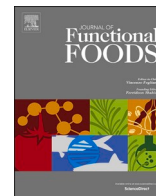
Uriel Urbizo-Reyes

Andrea M. Liceaga

Lavanya Reddivari

Kee-Hong Kim

Joseph M. Anderson

Enzyme kinetics, molecular docking, and *in silico* characterization of canary seed (*Phalaris canariensis* L.) peptides with ACE and pancreatic lipase inhibitory activity

Uriel Urbizo-Reyes [a,b], Andrea M. Liceaga [a,b,*], Lavanya Reddivari [b], Kee-Hong Kim [b], Joseph M. Anderson [c]

[a] *Protein Chemistry and Bioactive Peptides Laboratory, Purdue University, 745 Agriculture Mall Drive, West Lafayette, IN 47907, USA*
[b] *Department of Food Science, Purdue University, 745 Agriculture Mall Drive, West Lafayette, IN 47907, USA*
[c] *USDA-ARS, Department of Agronomy, Purdue University, 915 W. State St., West Lafayette, IN 47907, USA*

ARTICLE INFO

ABSTRACT

The bioactivity of canary seed peptides (CSP) towards metabolism-regulating enzymes was evaluated. Peptides with angiotensin-converting enzyme (ACE), dipeptidyl peptidase IV (DPP-IV), and pancreatic lipase activity remained stable ($p < 0.05$) to simulated gastrointestinal digestion (SGD). CSP-SGD were transported efficiently (>10%) through the Caco-2 monolayer, indicating absorption through the intestinal epithelium. Lineweaver-Burk plots demonstrated that CSP-SGD act as mixed-type inhibitors for DPP-IV and α-glucosidase. Furthermore, CSP-SGD were potent as antihypertensive and antiobesity agents. Molecular docking and *in silico* analyses were targeted to understand CSP-SGD interactions with ACE and pancreatic lipase. ACE-inhibitory peptides (LHPQ, QTPHQ, KPVPR, and ELHPQ) acted as non-competitive inhibitors by destabilization of the transition state and Zn(II) coordination in ACE. The uncompetitive inhibition of pancreatic lipase by peptides (VPPR, LADR, LSPR, and TVGPR) destabilized the open-lid conformation of pancreatic lipase. The results of this study showed that canary seed proteins could serve as a source of biologically active peptides.

1. Introduction

Obesity is considered a multifactorial pathology (environmental, social, behavioral, physiologic, psychological, and genetic) that originates from a disruption in the metabolic energy equilibrium, prompting an excess in energy intake (Heitkamp et al., 2021; Ray, Mahata, & De, 2016). Westernized populations are particularly vulnerable to suffer from obesity and overweight as a result of their social and dietary habits; this has become evident in the last 20 years, where countries like the USA have seen a spike from 30% to 42% in obesity (Kopp, 2019; CDC Centers for Disease Control and Prevention, 2020). Obesity is also considered to be the driving force towards development of chronic diseases such as diabetes, insulin resistance, inflammation, hypertension, among others (WHO, 2020b).

Chronic diseases arising from obesity could be prevented by the inclusion of a plant-based diet (WHO, 2020a). In addition, consumer concerns towards the use of synthetic drugs to treat chronic conditions has driven research to focus on natural or food derived constituents that offer similar health benefits but lack adverse side effects (Zhang, et al., 2021). Diets rich in vegetables protect against chronic diseases by lowering energy density, glycemic index, blood lipids, as well as improving insulin sensitivity, endothelial function, inflammatory, and oxidative stress conditions (Schwingshackl, Morze, & Hoffmann, 2020). Alternatively, some biological effects (e.g., antihypertension, antidiabetic, anti-inflammatory, antiobesity, and antioxidant) have been attributed to small molecular weight peptides originated from proteolysis and referred to as bioactive peptides (i.e., biopeptides). Typically, biopeptides are 2–20 amino acids long and their activity is affected by factors like amino acid sequence, molecular weight, hydrophobicity, and charge distribution (Karami & Akbari-Adergani, 2019; Zhang, et al.,

---

2021). Plant biopeptides could help decrease the incidence of hypertension, obesity, and diabetes by modulating key enzymes (e.g., ACE, DPP-IV, pancreatic lipase) that participate actively in specific pathologies (Daskaya-Dikmen, Yucetepe, Karbancioglu-Guler, Daskaya, & Ozcelik, 2017; Kumar, Narwal, Kumar, & Prakash, 2011; Sánchez & Vázquez, 2017). For instance, biopeptides from hemp, quinoa, and common bean have shown inhibitory activity against angiotensin converting enzyme (ACE), dipeptidyl peptidase IV (DPP-IV), α-glucosidase, and pancreatic lipase (Awosika & Aluko, 2019; Nongonierma, Le Maux, Dubrulle, Barre, & FitzGerald, 2015; Orio et al., 2017; Vilcacundo, Martínez-Villaluenga, & Hernández-Ledesma, 2017). In this context, emerging or novel plants with high protein content are of particular interest to scientists as they could represent a high source of biopeptides and could be used to formulate functional foods and nutraceuticals.

Hairless canary seed (*Phalaris canariensis* L.) is considered as a novel plant with high protein content (19–24%) used in traditional medicine to treat various chronic diseases (Valverde, Orona-Tamayo, Nieto-Rendón, & Paredes-López, 2017). For example, they have served as a traditional remedy in Mexico to treat obesity, diabetes, and hypertension (Estrada-Salas, Montero-Morán, Martínez-Cuevas, González, & Barba de la Rosa, 2014), supporting their potential application for human consumption as a novel food ingredient (Patterson, et al. 2018, Mason, L'Hocine, Achouri, & Karboune, 2018). Preliminary research from our group has indicated that biopeptides from the proteolysis of canary seed protein have the ability to inhibit enzymes (α-glucosidase, ACE, DPP-IV, and pancreatic lipase) (Urbizo-Reyes, Aguilar-Toalá, & Liceaga, 2021). The ability of biopeptides to exert an effect *in vivo* depends strongly on their gastrointestinal stability and their ability to cross the intestinal epithelium (Bhandari et al., 2020). So far, information involving the specific peptide sequences, bioavailability, and the molecular interactions (peptide-enzyme) of canary seed biopeptides is unknown. Therefore, the aim of this study was to evaluate the *in vitro* gastrointestinal stability and bioavailability of canary seed peptides, identify the peptides sequences involved in biological activities, and understand their mechanism of action using enzyme kinetics and molecular docking strategies. In this study, we assessed the bioactivities of simulated gastrointestinal digested canary seed peptides, implemented enzyme kinetics, and fractionated the peptides. *In silico* analysis of identified fractions was applied to identify relevant structural characteristics and the molecular interaction of these biopeptides (ligands) with their most potent receptors (ACE and pancreatic lipase).

2. Materials and methods

2.1. Materials

Hairless canary seeds (CDC Cibo) were purchased from a commercial vendor (Can-pulse Foods LTD, Saskatoon, SK, Canada). Alcalase® (protease from *Bacillus licheniformis*), was purchased from Novozymes (Bagsvaerd, Denmark). Pancreatic lipase (Type VI-S ≥ 20,000 units/mg protein, EC 3.1.1.3), rat intestinal acetone powder (α-Glucosidase, EC 3.2.1.20), angiotensin-converting enzyme (ACE; ≥10 units/mg protein, EC 3.4.15.1), dipeptidyl peptidase-IV (DPP-IV, ≥ 4500 units/ μg protein, EC 3.4.14.5) and their substrates oleic acid 4-methylumbelliferyl ester, p-nitrophenyl-α-d-glucopyranoside, Gly-Pro p-nitroanilide hydrochloride, and hip-puryl-L-histidyl-L-leucine (HHL), respectively, were all purchased from Millipore Sigma (St. Louis, MO, USA). Caco-2 cells were purchased from Millipore Sigma (St. Louis, MO, USA). Chemicals and materials not specified above were purchased from companies VWR

International (Radnor, PA, USA), Millipore Sigma (St. Louis, MO, USA), and Thermo Fisher Scientific (Waltham, MA, USA).

2.2. Preparation of canary seed peptides (CSP) and simulated gastrointestinal digestion (SGD)

Canary seeds were defatted by cold mechanical oil extraction (37 ± 2 °C), crushed, and hydrolyzed following the methodology detailed by Urbizo-Reyes et al. (2021). Briefly, defatted canary seed powder was diluted (22.5 mg of protein/mL) and homogenized in deionized water using Sorvall Omni Mixer with a macro-attachment assembly (Norwalk, CT, USA). The solution's pH was adjusted to 8.0 with 2 M NaOH and preheated to 50 ± 3 °C followed by hydrolysis for 4 h with 3% (w/w) Alcalase®. Hydrolysis was terminated by heat treatment (95 ± 3 °C) for 15 min. The solution was cooled and centrifuged (17,636g for 15 min) (Avanti J-26S Centrifuge, Beckman-Coulter INC. CA, USA). The supernatant was collected as soluble peptides and stored at −80 °C until use.

Next, the peptides were subject to simulated gastrointestinal digestion (SGD) using a modified method described by Minekus et al., (2014). Briefly, the peptides solution (10 mg of protein/mL) was adjusted to pH 2.0 using 1 M HCl and incubated with pepsin (4% w/w of protein) at 37 °C for 2 h. Then, 0.9 M NaHCO₃ was used to adjust pH to 5.3, and 1.0 M NaOH to further increase the pH to 7.5. Pancreatin was then added (4% w/w of protein), and the mixture incubated at 37 °C for 2 h. The digestion was terminated by pasteurization (95 ± 3 °C) for 15 min. Subsequently, the solution was cooled to room temperature and centrifuged at 11,000g for 15 min; the supernatant was collected and referred to as digested peptides. Preliminary studies showed that small peptides (<3 kDa) from canary seed were the most biologically active (Urbizo-Reyes et al., 2021). For this reason, peptides were fractionated by ultrafiltration using a <3 kDa cutoff membrane and referred to as canary seed peptides (CSP) and CSP after simulated gastrointestinal digestion (CSP-SGD), respectively. Lastly, CSP and CSP-SGD were frozen at −80 °C for 12 h and freeze-dried using a Labconco FreeZone Plus 2.5 L cascade benchtop freeze dry system (Labconco Corp., Kansas City, MO). The powders were stored at 4 ± 1 °C until analysis. The peptide content was normalized using the bicinchoninic acid (BCA) protein assay (Thermo Scientific, Rockford, IL, USA) before subsequent analysis.

2.3. α-Glucosidase inhibitory activity

The inhibition of α-glucosidase activity was determined as described by Sultana et al., (2020). Initial, α-glucosidase was extracted by solubilizing 300 mg of intestinal acetone powder from rat in 9 mL sodium chloride solution (0.9% w/v) and vortexed for 5 min. Then, the solution was centrifuged at 12,500g for 5 min, the supernatant was recovered and used as a source of α–glucosidase (8.33 mg/L). Briefly, a 50 μL aliquot of sample suspended in 0.1 M sodium phosphate buffer (pH 6.9) was pipetted into a 96-well microplate, with 50 μL of α-glucosidase, followed by a pre-incubation for 10 min at 37 °C. Next, the reaction was initiated by pipetting 100 μL of 4-nitrophenyl α-D-glucopyranoside (5 mM). The inhibition was calculated spectrophotometrically using Multiskan™ FC Microplate Photometer (Waltham, MA, USA), reading the absorbance at 405 nm for 30 min. Acarbose was used as a reference. The percentage inhibition was calculated using equation [Eq. (1)].

$$\alpha\text{-}glucosidase\ inhibition\ (\%) = 100 \times \left[\frac{Abs\ Control\ (no\ inhibitor) - Abs\ Sample}{(Abs\ Control\ (no\ inhibitor)}\right] \tag{1}$$

2.4. Determination of ACE inhibitory activity

ACE-inhibitory activity was measured according to the method described by Urbizo-Reyes, et al. (2019). Peptide samples (CSP and CSP-SGD) were dissolved in phosphate buffer (100 mM, pH 8.3) with 300 mM sodium chloride. Aliquots (25 μL) of peptide sample solutions were added to 25 μL of the substrate hippuryl-L-histidyl-L-leucine (HHL) and incubated at 37 °C for 4 min. Aliquots (80 μL) of human-ACE (50 mU) were added to initiate the reaction, followed by incubation at 37 °C in a water bath with constant stirring for 2 h. The reaction was terminated by adding 50 μL of 1 M HCl and diluted by adding 50 μL of acetonitrile solution with 1% (v/v) trifluoroacetic acid (TFA) and 50 μL of distillated water with 1% (v/v) TFA. A control reaction was performed using 25 μL of the buffer instead of the inhibitor (CSP). Hippuric acid (HA) was quantified using high-pressure liquid chromatography (HPLC) (Model 600E, Waters Corporation, Milford MA) with a C18 analytical column (YMC Pack ODS AM 12505-2546 wt, YMC America, Inc., Allentown, PA, USA). The commercial drug captopril was used as positive control. Finally, percent inhibition was calculated using equation [Eq. (2)].

$$ACE\ inhibition\ (\%) = [1 - \frac{A\_inhibitor}{A\_control}] \times 100 \qquad (2)$$

where *A_inhibitor* and *A_control* represent the relative areas (A) with and without inhibitor of the HA peaks.

2.5. Dipeptidyl peptidase IV (DPP-IV) inhibitory activity

The DPP-IV inhibitory activity of the samples was determined following the method by Hall et al. (2018). Briefly, 25 μL of the peptide samples dissolved in 100 mM Tris-HCl buffer (pH 8.0) were pre-incubated in a 96-well microplate with 25 μL of substrate Gly-Pro p-nitroanilide hydrochloride (6 mM) at 37 °C for 10 min. Then, 50 μL of human DPP-IV (4.5 U/mL) was added, followed by incubation at 37 °C for 60 min. The reaction was stopped by adding 100 μL of 1 M sodium acetate buffer (pH 4.0). Absorbance of released p-nitroanilide was measured at 405 nm using a Multiskan™ FC Microplate Photometer (Waltham, MA, USA). The sample blank (no inhibitor) used buffer instead of the sample. For the negative control (no DPP-IV activity), the buffer was used instead of DPP-IV solution. Percent DPP-IV inhibition was calculated using equation [Eq. (3)].

$$Inhibition\ (\%) = \left[1 - \frac{(Abs\ sample - Abs\ sample\ blank)}{(Abs\ positive\ control - Abs\ negative\ control)}\right] \times 100 \qquad (3)$$

2.6. Pancreatic lipase inhibition

Pancreatic lipase inhibition activity was measured following the methodology by Zhu et al. (2014) with modifications. Briefly, samples, substrate, and pancreatic lipase were dissolved in McIlvaine buffer (0.1 M Citrate-Na2HPO4, pH 7.4). Then, 50 μL of substrate 4-methyl-umbelliferyl oleate (1 mM) was pre-incubated with 25 μL of peptide sample for 10 min in a black 96-well microplate. The reaction was started by adding 25 μL of pancreatic lipase type-VI (200 U/mL) and carried out for 1 h. The production of 4-methylumbelliferone was measured fluorometrically using a Fluoroskan Ascent FL Microplate Fluorometer and Luminometer (ThermoFisher Scientific, Waltham, MA, USA) using an excitation wavelength of 355 nm and emission wavelength of 460 nm. Sample absorbance was corrected by subtracting blanks in which pancreatic lipase was replaced with McIlvaine buffer. The sample blank (no inhibitor) used the buffer instead of the sample. Instead of pancreatic lipase solution, the buffer was used as negative control (no pancreatic lipase activity) and the commercial drug orlistat was used as the positive control. Finally, lipase inhibition was calculated using equation [Eq. (3)].

2.7. Mode of inhibition using enzyme kinetics

The mode of enzyme inhibition was calculated by measuring the inhibitory capacity of CSP-SGD peptides at various substrate concentrations and calculating the initial reaction velocities from the product formation over time (Hall et al. 2018). The CSP-SGD and the substrates concentrations used in this study were: (0, 4 and 8 mg/mL) of CSP-SGD and (0.625, 1.25 2.5 and 5 mM) of 4-nitrophenyl for α-D-glucopyrano-side α-Glucosidase; (0, 0.5 and 1 mg/mL) of CSP-SGD and (1.25, 2.5, 5, 10 mM) of HHL for ACE; (0, 5, and 10 mg/mL) of CSP-SGD, and (2, 4, 6, and 8 mM) of Gly-Pro p-nitroanilide hydrochloride for DPP-IV; (0, 1, and 2 mg/mL) of CSP-SGD, and (1, 2, 3 and 4 mM) of 4-methylumbelliferyl oleate for pancreatic lipase. Enzyme inhibition (%) was measured as described above. Reaction velocities were determined from the formation of the product over time as (ΔAbs/min) or (Δarea/min). Finally, Km, Vmax and type inhibition were assessed by Lineweaver-Burk graphs using the reciprocal of product concentration versus the reciprocal of substrate concentration at various CSP-SGD concentrations.

2.8. Reverse-Phase-High-Performance-Chromatography (RP-HPLC)

CSP-SGD were further purified utilizing as detailed by Nuchprapha et al. (2020). Briefly, CSP-SGD was suspended in HPLC grade deionized water and filtered (0.45 μm). A volume of 50 μL of CSP-SGD (7 mg protein/mL) was injected at 25 °C to a XBridge™ BEH130 C18 column (10 μm, 10 × 150 mm, Waters Inc., Milford, MA, USA) using a two-stage gradient procedure: starting with an eluent concentration of 100:0% (v/v) A: B decreasing to 75:25% (v/v) A: B over 35 min, and then to 60:40% (v/v) A:B over 60 min, at a flow rate of 0.3 mL/min. Mobile phase A consisted of HPLC grade deionized water with 0.1% (v/v) TFA, while B was HPLC grade acetonitrile with 0.1% (v/v) TFA. The process was carried out using a Waters 2690 HPLC system (Waters Corporation, Milford, MA, USA), equipped with an automatic sample injector and 2998 UV photodiode array (PDA) detector. The elution of peptide fractions was monitored at a wavelength of 280 nm. The eluted fractions (F1-F7) (Supplementary Materials Fig. 1S) were collected, concentrated, and stored at –80 °C until analysis. Based on the results of sections 2.3–2.7, the fractions were further tested for their most potent biological properties (ACE and pancreatic lipase inhibitory activities).

2.9. Transport study using Caco-2 monolayer

The bioavailability of the CSP-SGD was evaluated according to Dueik and Bouchon (2016). CSP-SGD were centrifuged, and the supernatant filtered using a 0.45 μm syringe filter. The supernatant was used to assess the transport across intestinal epithelial cells. Briefly, Caco-2 cells (22–27 passages) were grown in tissue culture flasks with Eagle's Minimum Essential Medium (EMEM) supplemented with 10% fetal bovine serum, 100 U/L of penicillin, 50 μg/ml gentamicin (CMEM), 100 μM of non-essential amino acids, and 100 U/L of streptomycin. Cells were grown at 37 °C under an atmosphere containing 5% CO₂. The medium was changed every 2- days, and the cells sub-cultured weekly by trypsin-EDTA treatment. Then, the monolayer was developed by seeding in 6-well high pore density polyethylene terephthalate inserts at a density of 2.5×10^5 cells per cm^2 and growing the cells for 20–21 days, replacing the medium every 2 days. The permeability of lucifer yellow (0.1 mg/mL) was measured before and after the experiment, and only wells with a permeability below 3% were used in the experiment. Next, the cells were washed twice using HBSS buffer (pH 7.2) and incubated for 30 min each time before starting the experiment. Finally, the CSP-SGD was added to the apical layer at a concentration of 4.5 mg/mL and incubated as described above. After 2 h, samples from the apical and basolateral layers were collected and freeze-dried. The apical (50 μL) and baso-lateral (50 μL) constituents were injected into an analytical C18 column.

Samples were analyzed by RPH-HPLC, eluted using a linear gradient of acetonitrile (0–60% in 30 min) and 0.1% TFA in H$_2$O at a flow rate of 0.5 mL/min, at an absorbance of 214–280 nm. The transport percentage was calculated by measuring the peak areas of the original test peptides (apical) and the overall amount of the original peptide plus degradation products transported through the monolayers (basolateral).

2.10. Identification of ACE and pancreatic lipase inhibitory peptides

The most active peptide fraction was selected for tandem-mass spectrometry (LC-MS/MS) and de novo sequencing in collaboration with the Proteomics Core facility at the Indiana University School of Medicine (Indianapolis, Indiana, USA) following methods described by Hall, Reddivari, and Liceaga (2020). Briefly, 200 µg of CSP-SGD (from fraction F7) were suspended in 100 µL 0.1% formic acid, then 10 µL were injected into a 5 cm trap column and a 15 cm (2 µm particle size, 50 µm diameter) EasySpray (801A) column on an UltiMate 3000 HPLC and Q-Exactive Plus (ThermoFisher Scientific, Walthman, MA, USA) mass spectrometer. Data analysis was performed using the PEAKS Xpro de novo software (Bioinformatics Solutions). Only peptides with de Average Local Confidences scores > 80% were selected to be further processed for molecular docking analysis. The Thermo Fisher Peptide analyzing tool server (available at https://www.thermofisher.com/us/en/home/life-science/protein-biology/peptides-proteins/custom-peptide-synthesis-services/peptide-analyzing-tool.html) was utilized for determination of physiochemical properties (e.g., GRAVY, hydrophobicity, PI) of identified peptides and BIOPEP-UWM server (http://www.uwm.edu.pl/biochemia/index.php/en/biopep) was implemented for database search for bioactive peptide sources (Minkiewicz, Iwaniak, & Darewicz, 2019). Then, ACE inhibitory peptides were further filtered by *in silico* prediction algorithms of antihypertensive peptides using the AHTPin online server at (available at http://crdd.osdd.net/raghava/ahtpin/) for antihypertensive potential using a scoring function, where a score above 0 indicates the peptide has antihypertensive potential and score below 0 indicates poor antihypertensive potential (Bounouala, Roudj, Karam, Recio, & Miralles, 2017). Based on this scoring (SVM > 0.9) the best 30 peptides were selected for molecular docking analysis. Similarly, pancreatic lipase inhibitory peptides were subject to a second round of filtration based on literature criteria in the following scheme: arginine content in peptide sequence (Stefanucci et al., 2019), and hydrophobic amino acid score (Mudgil, Kamal, Yuen, & Maqsood, 2018), thus, selecting the top 20 peptides for molecular docking analysis.

2.11. Molecular docking of canary seed biopeptides

Molecular docking was performed with AutoDock Vina as previously described by Hall et al. (2020). BIOVIA Discovery Studio® 4.5 Visualizer (BIOVIA Corporate Americas, San Diego, CA, USA) was utilized to construct CSP-SGD peptides, then charges were added to the molecules and the optimal conformations were identified by energy minimization by Merck Molecular Force Field (MMFF94) utilizing ChemBiodraw 3D (PerkinElmer, MA, USA). Discovery Studio software and AutoDock4 (4.2.6) were used for enzyme preparation prior to docking and to visualized peptide-protein interactions (Trott, & Olson, 2010). First, ACE (PDB ID: 1O8A) and pancreatic lipase (PDB ID: 1ETH) 3D crystal structures were prepared for docking by removing Linosinopril, hydroxyethyloxy triethyloxy, and water molecules (Hermoso, Pignol, Kerfelec, Crenon, Chapus, & Fontecilla-Camps, 1996; Natesh, Schwager, Sturrock, & Acharya, 2003). Then polar hydrogen atoms and cofactors like Zn^{2+} interacting with E411 D415 H383 and H387 and chloride ions were added when applicable, then the binding sites coordinates were defined as x = 41.194, y = 33.848, z = 46.304 with a radius of 60 Å for ACE, and x = 71.524, y = 26.883, z = 187.849 with a radius of 60 Å for pancreatic lipase. Inhibitor drugs orlistat and captopril were downloaded from the drug bank website (https://www.drugbank.ca/) and utilized as positive control for molecular docking analysis. Then, the

best-ranked docking modes (Supplementary Materials Table 1S and 2S) were selected according to the affinity energy values, and peptide-enzyme interaction figures were analyzed and developed using Discovery Studio 2021 visualizer (Accelrys Software Inc., San Diego, CA, USA; Discovery Studio Modeling Environment, Accelrys Software Inc., San Diego, CA, USA, 2016).

2.12. Statistical analysis

The results in this study were analyzed using a complete randomized design, analyzed with a One way-ANOVA under Tukey ($p < 0.05$) by the statistical software SAS 9.4® (Cary, NC, USA). Results were reported as mean ± standard deviation (SD) of triplicate determinations.

3. Results and discussion

3.1. Impact of SGD on enzyme inhibition capacity

Previously, we demonstrated that canary seed peptides (CSP) with molecular weight < 3 kDa showed high potential for biological activity towards enzymes related to obesity, diabetes, hypertension, and oxidative stress (Urbizo-Reyes et al., 2021). This bioactivity has been reported in other plant proteins and attributed to the exposure of aromatic, charge, and hydrophobic amino acids that are liberated from the protein core that react with these enzymes (Ketnawa, Suwal, Huang, & Liceaga, 2018; Nongonierma, et al., 2015; Urbizo-Reyes et al., 2019). To understand the bioactive stability of CSP to gastrointestinal digestion, the inhibitory activity of < 3 kDa CSP and CSP after simulated gastrointestinal digestion (CSP-SGD) fractions was tested against chronic disease-related enzymes such as α-glucosidase, ACE, DPP-IV and pancreatic lipase. After SGD, the half-maximal inhibitory (IC$_{50}$) concentration increased ($p < 0.05$) for α-glucosidase from 1.15 to 1.47 mg/mL (Fig. 1). These results are similar to those reported for peptides produced by hydrolysis with Alcalase of orange seed (*Siavaraze, Citrus sinensis*) and hemp seeds (*Cannabis sativa* L), which showed a decrease in α-glucosidase inhibition after SGD (Mazloomi et al., 2020; Ren et al., 2016). This could be a result of the digestion of the active peptide fractions, causing a loss in bioactivity. *In silico* tools corroborated this theory, showing that peptides from different sources (including *Aspergillus awamori*, albumin, and egg white protein) with high to moderate α-glucosidase inhibitory activity were unstable to gastrointestinal digestion (Ibrahim, Bester, Neitz, & Gaspar, 2018).

Conversely, this was not the case for ACE and DPP-IV inhibition, where there was no significant change observed for inhibition of ACE and DPP–IV after SGD, indicating gastrointestinal stability. Based in the *in silico* analysis, the ACE inhibitory peptides identified from the CSP-
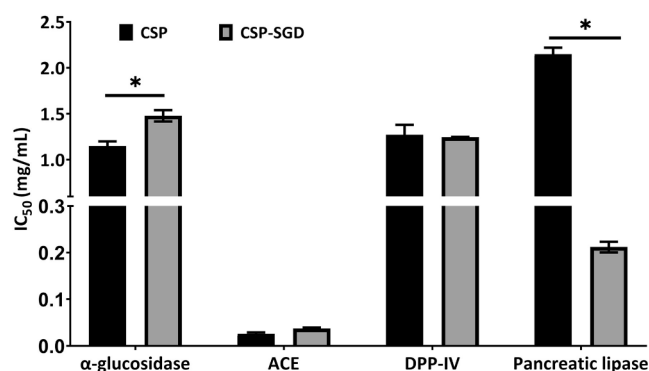

Fig. 1. α-Glucosidase, ACE, DPP-IV, and pancreatic lipase inhibition of canary seed peptides (CSP) and canary seed peptides after simulated gastrointestinal digestion (CSP-SGD). Bars represent mean values of triplicate determinations ± standard deviation. Asterisks (*) indicate statistical differences ($p < 0.05$) between CSP and CSP-SGD.

SGD had a high content of proline residues in their last and penultimate position (Supplementary Materials Table 1S). This characteristic is reported to make peptides less susceptible to proteolytic enzymes, allowing them to resist gastrointestinal digestion (Hall et al., 2020). Similarly, amino acid composition and chain length could have prevented DPP-IV inhibitory peptides from degrading during SGD. This hypothesis is supported by studies conducted on collagen (Wang et al., 2021) and whey (Nongonierma & FitzGerald, 2013) peptides, where factors like small molecular weight (4–5 amino acids), and intermediate proline content increased the tendency of DPP-IV inhibitory peptides to resist gastrointestinal digestion. Additionally, the specific positioning of rigid amino acids like proline near aromatic and basic amino acids can confer a peptide resistance to digestion by pepsin and trypsin (De Angelis, et al., 2021). This study's DPP–IV inhibition results (1.24 mg/mL) also align with those reported by Estrada-Salas et al. (2014) for peptides from canary seed; however, the ACE inhibition of the CSP-SGD was much higher (0.037 mg/mL) than those reported by Estrada-Salas et al. (2014) for canary seed peptides after gastrointestinal digestion (0.332 mg/mL).

The IC$_{50}$ values for pancreatic lipase inhibition decreased (p < 0.05) after SGD (Fig. 1). Stefanucci et al. (2019) discovered that arginine-rich proteins highly inhibit this lipase. In agreement with this, canary seed protein has a notoriously high content of arginine (6.4%, w/w dry basis of protein) when compared to other cereals like wheat (5.1%), oat (5.79%), barley (4.6%), and millet (3.9%) (Mason, L'Hocine, Achouri, & Karboune, 2018). Furthermore, the proximity of arginine to the C-terminal of the peptide chain could increase pancreatic lipase inhibitory capacity (Stefanucci et al., 2019). In this context, peptides subject to gastrointestinal digestion increased their activity due to the exposure of arginine residues in the last and penultimate position of their amino acid chain (Supplementary Materials Table 2S). This event is caused by the digestion with trypsin, which cleaves C-terminal arginine, and lysine, yielding a high abundance of arginine in the aforementioned sites. Overall, these results indicate that canary seed peptides hold good biological activity even after being exposed to gastrointestinal conditions, and could potentially serve as functional or nutraceutical ingredients.

3.2. Mode of inhibition of CSP-SGD

Lineweaver–Burk plots were created to determine the mode of

inhibition of the CSP-SGD biopeptides by assessing the α-glucosidase, ACE, DPP-IV, and pancreatic lipase inhibition at various peptide and substrate concentrations (Fig. 2). Data showed that the K$_m$ (x-axis) of the α-glucosidase and DPP-IV changed while the V$_{max}$ (y-axis) decreased as the CSP-SGD concentration increased; this indicates that CSP-SGD acted mainly as mixed-type inhibitors. In the case of ACE, we can observe no changes in K$_m$, but a drop in V$_{max}$ as the peptide concentration increased; this indicates that the peptides act as non-competitive inhibitors. Surprisingly, an increase in CSP-SGD seemed to cause a decrease in both K$_m$ and V$_{max}$ for pancreatic lipase, resulting in a parallel pattern on the plots, associated with an uncompetitive inhibition (Moreno-Córdova et al., 2020).

Until now, there was no information on the mode of inhibition of peptides from canary seed towards chronic disease-related enzymes (α-glucosidase, DPP-IV, ACE, and pancreatic lipase). The Lineweaver-Burk double reciprocal plots indicated that CSP-SGD acted as mixed-type inhibitors for α–glucosidase and DPP-IV. Mixed type inhibitors affect the binding of the substrate and the velocity of catalysis of the enzymatic reaction, allowing the peptides to bind to both free enzyme and substrate-enzyme complexes with slight variation in affinity energies (Ring, Wrighton, & Mohutsky, 2014). For ACE, the outcomes indicate a non-competitive type of inhibition. Non-competitive inhibitors usually have a reversible binding nature and does not affect the substrate-binding process, as they could act on various sites to induce conformational changes that affect enzyme activity (Ring et al., 2014). Conversely, CSP-SGD displayed an un-competitive mode of inhibition towards pancreatic lipase. This mechanism of action relies on the inhibitors binding only to enzyme-substrate complexes, inducing conformational stages that prevent the enzyme from functioning correctly (Ring et al., 2014).

3.3. Transport study, ACE and pancreatic lipase inhibition of CSP-SGD peptide fractions

To further understand the biological potential of CSP for human health, we assessed their transport through the epithelium, stability to gastrointestinal digestion, and determined amino acid sequence of the most active peptide fraction. RP-HPLC was used to separate CSP-SGD into seven fractions (Supplementary Materials Fig. 1S). The percentage inhibition of ACE and pancreatic lipase and the transport across
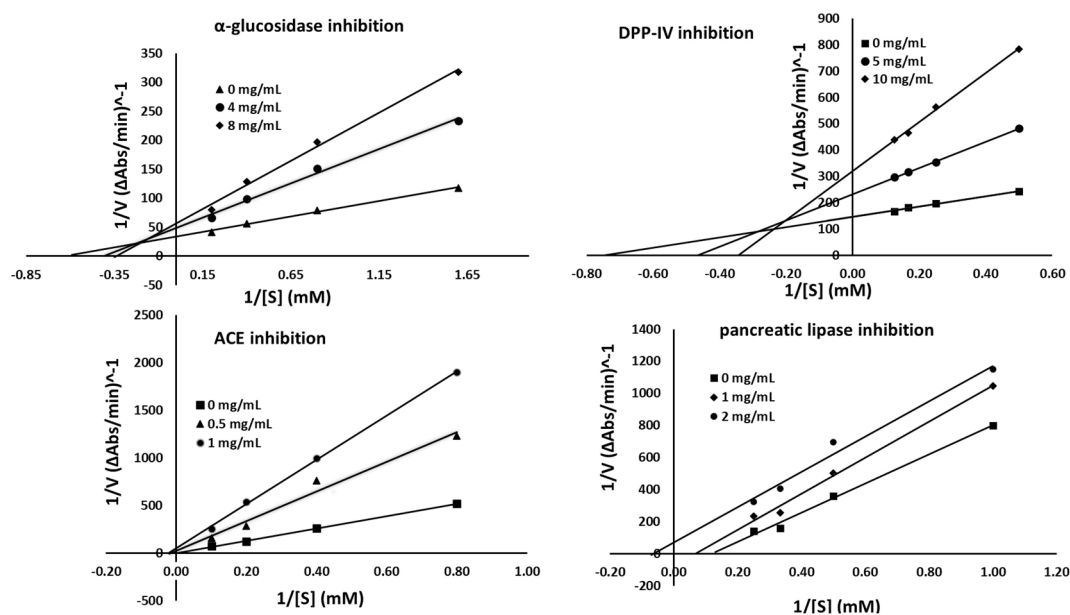
Fig. 2. Lineweaver-Burk plot of α-Glucosidase, ACE, DPP-IV and pancreatic lipase enzymes by canary seed peptides after simulated gastrointestinal digestion (CSP-SGD).
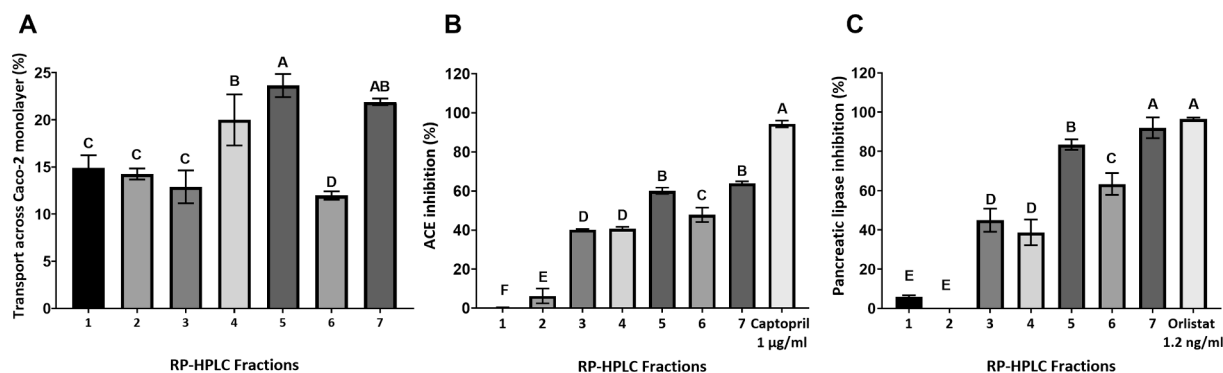
Fig. 3. Transport (%) of canary seed peptide fractions (F1-F7) across Caco-2 monolayer (A) after simulated gastrointestinal digestion (CSP-SGD), and their inhibition activity against ACE (B), and pancreatic lipase (C). Peptide fractions were collected by RP-HPLC (normalized to a protein concentration of 35 μg/mL). Bars represent mean values of triplicate determinations ± standard deviation. Different letters (A-F) indicate statistical differences (p < 0.05) between fractions.

Caco-2 monolayer for CSP-SGD fractions F1-F7 are shown in Fig. 3. All CSP-SGD fractions had a bioavailability > 10% (Fig. 3A), with higher (*p* < 0.05) capacity to be transported observed for fraction F5 (23.64%) and F7 (21.89%), followed by F4, F3, F2, F1, and the lowest transport for F6. Caco-2 permeation leads to the formation of new peaks and peak shoulders that might be the product of cellular digestion (Supplementary Materials Fig. 2S). It is known that peptides can be transported via the PepT1 and paracellular transport pathways through the intestinal epithelium, where factors like charge, hydrophobicity, composition, and position of the amino acids could impact their transport rates (Wang, Xie, & Li, 2019). For instance, scientific literature reports that peptides with different chain lengths can be absorbed through different routes such as PepT1-mediated transport for di- and tri-peptides, the passive paracellular route for oligopeptides with < 8 amino acids, and the transcytosis route for long-chain peptides with < 10 amino acids (Aguilar-Toalá & Liceaga, 2021; Xu, Hong, Wu, & Yan, 2019). The small molecular weight of the peptides identified in this study (316–1753 Da) (Supplementary Materials Table 3S) and the differences in hydrophobicity profile of the peptide fractions (F1-F7) could contribute to the observed transport yields. For example, peptides (1437 Da) from bovine milk permeated up to 38% through Caco-2 monolayer (Picariello et al., 2013). In another study, oligo peptides from collagen with molecular weights (1000 and 200 Da) permeated around 13% and 23%, respectively (Song, Tian, & Li, 2020). In the case of hydrophobicity, this could have accounted for the high transport rate of F7. From this respect, it is reported that highly hydrophobic peptides bind firmly to PepT1 (Newstead, 2015). The positive correlation of peptide hydrophobicity with permeability across the Caco-2 monolayer has been widely validated in literature (Bao, Zhao, Wang, Chi, & Technology, 2017; Xie, Wang, Jiang, Liu, & Li, 2015). Hydrophobic peptides are likely transported by diffusion and their counterparts by carrier-mediated and energy-dependent processes that could facilitate their transport and rationalize the intensification of transport yields for sequences eluting last during RP-HPLC (Xie et al., 2015).

The bioactivity of the peptide fractions increased as the elution progressed, and all collected fractions displayed high capacity to inhibit ACE and pancreatic lipase (>40%), except for fractions F1 and F2 (Fig. 3B). As expected, the positive control captopril (1 μg/mL) showed a significantly (*p* < 0.05) higher inhibition capacity (94%) towards ACE than any other peptide fraction. Nevertheless, fractions F7 and F5 (35 μg/mL) were the most active (*p* < 0.05), inhibiting ACE by 64% and 60%, respectively. Similarly, F7 (35 μg/mL) had the highest (*p* < 0.05) pancreatic lipase inhibitory activity (92%) and in this case, it was as effective as the positive control orlistat (1.2 ng/mL) with 96% inhibition (Fig. 3C). This observation is believed to be a result of the higher content of hydrophobic peptides present in latter eluted fraction (F7) (Supplementary Materials Table 3S). Hydrophobicity has shown to be a relevant structural parameter that could modulate a peptide's biological activity

(Karami & Akbari-Adergani, 2019). It is known that peptides separated with RP-HPLC result in hydrophobic peptide fractions being eluted last (Montone, et al., 2019). Likewise, studies on sunflower, (Megías et al., 2009), wheat (Liu et al., 2021), and longan seeds (Nuchprapha et al., 2020) have demonstrated similar results, where fractions separated with RP-HPLC that eluted last had the highest biological activity. To gain mechanistic insights of the CSP-SGD interaction with ACE and pancreatic lipase, we used LC-MS/MS analysis and a molecular docking simulation of the most active fraction (F7).

3.4. Identification and molecular docking analysis of CSP-SGD with ACE inhibition

About 56% of the peptides from fraction F7 were predicted to exhibit antihypertensive potential (SVM score > 0.0), and 69 peptides showed high antihypertensive potential (SVM score > 0.9), of which the four peptides (LHPQ, QTPHQ, KPVPR, and ELHPQ) with the highest binding activity towards ACE are shown in Fig. 4. Database search using BIOPEP-UWM online server (http://www.uwm.edu.pl/biochemia/index.php/en/biopep, accessed 5/28/2021) revealed that canary seed peptides had in their sequences di- and tri-peptides previously reported with ACE-inhibitory activity (e.g., PLP, VPP, HL, HP, QP, and KP) (Minkiewicz, Iwaniak, & Darewicz, 2019). These four peptide sequences had binding energies (Affinity Energy) ranging from −8.9 to −8.0 kJ/mol, negative GRAVY (average hydrophobicity and hydrophilicity) scores (−2.5 to −1.1) indicating high hydrophobicity, and holding interactions sporadically with 11 main residues of the ACE structure (Table 1). Overall, CSP-SGD (F7) interacted with ACE residues mainly by hydrogen bonding, followed by Van der Waals, and hydrophobic interactions with a lower contribution of metal bonding, and electrostatic interaction by salt bridges. Molecular docking analysis revealed inhibitory motifs of CSP-SGD (F7), which were especially rich in proline, glutamine, and cationic residues (lysine and histidine) (Fig. 4 and Supplementary Materials Table 1S).

Proline-rich peptides LHPQ and KPVPR exhibited hydrophobic interactions, playing an essential role in the interaction with ALA 354, HIS353/383, PHE457, and VAL380. Glutamine-rich peptides QTPHQ and ELHPQ interacted in a higher frequency by hydrogen bonding and salt bridges (electrostatic interactions) with ALA354, ASN277, GLN281, GLU162/384, HIS353/513, LYS511, and ZN (II) with a significant role in the peptide enzyme interaction. In the case of cationic residues (lysine, arginine, and histidine), they interact mainly by conventional hydrogen bonding with a less frequent amount of electrostatic and hydrophobic interactions with ALA354, ASP453, GLU162, HIS353/513, and VAL379/380 (Fig. 4).

The hydrophobic amino acid proline and its proximity to the C-terminal has been directly associated with ACE-inhibition (Ianzer et al., 2007; Hall et al., 2020). This agrees with the results observed in our
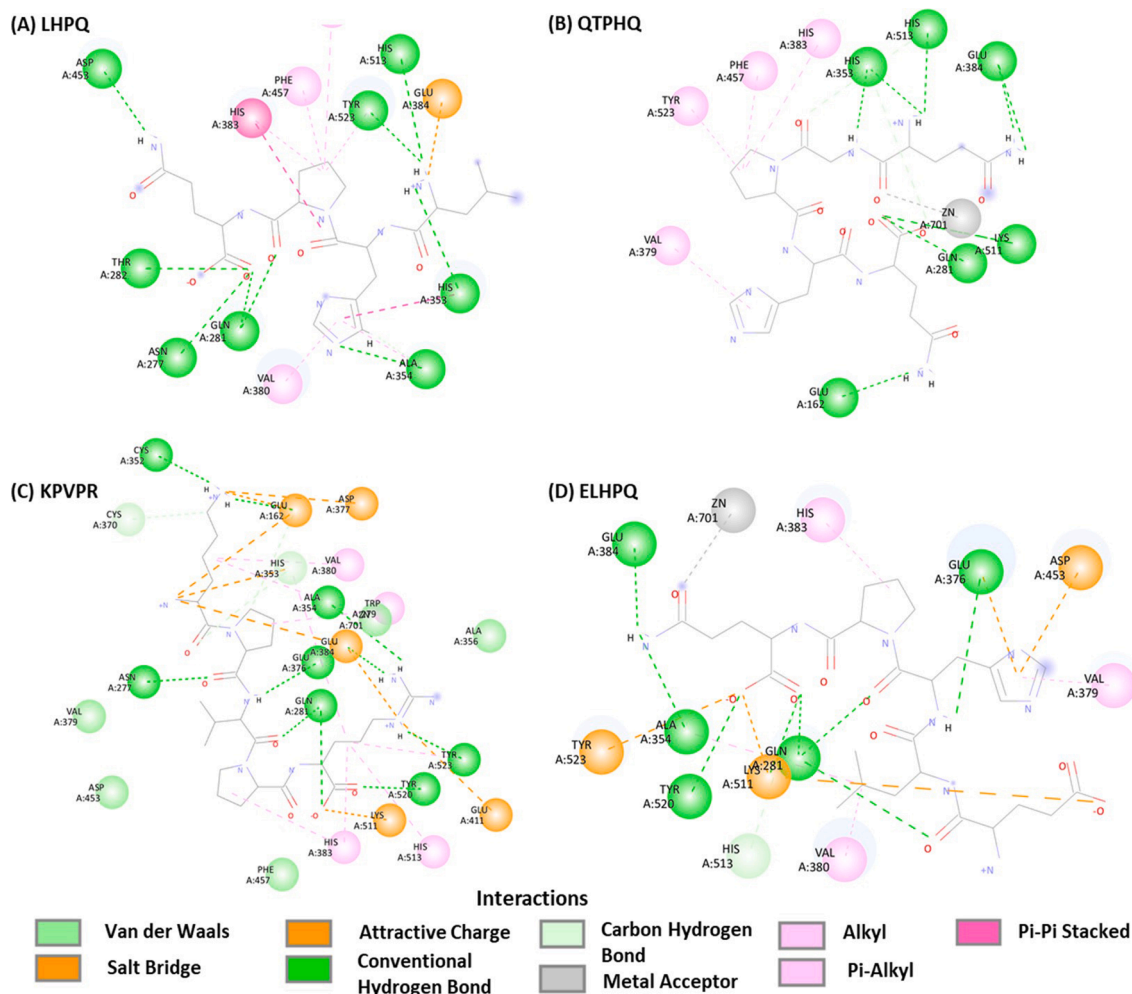
Fig. 4. Interaction of four canary seed peptide sequences (A-D) with the highest binding energy towards angiotensin converting enzyme (ACE).

Table 1
Binding energies and interacting residues of docked canary seed peptides identified by LC-MS/MS.

ACE inhibitory peptides					Pancreatic lipase inhibitory peptides				
Peptide attribute	LHPQ	QTPHQ	KPVPR	ELHPQ	Peptide attribute	VPPR	LADR	LSPR	TVGPR
Affinity Energy (kJ/mol)	−8.9	−8.6	−8.2	−8.0	Affinity Energy (kJ/mol)	−6.2	−6.0	−6.0	−5.9
de novo Score (%)	96	86	87	89	de novo Score (%)	92	97	95	85
Mass (Da)	493.6	609.7	595.8	622.7	Mass (Da)	454.3	494.2	484.3	442.2
Hydrophobicity	4.8	2.3	5.1	5.9	Hydrophobicity	3.0	2.4	5.5	4.3
GRAVY	−1.1	−2.5	−1.5	−1.6	GRAVY	−0.9	−0.6	−0.8	−0.6
ACE interacting residues					**Pancreatic lipase interacting residues (Step 1–4)[1]**				
ALA354	+	+	+	+	ASP248 (S1)	+	+	+	−
GLU162	−	+	+	−	ASP250 (S1)	+	−	+	−
GLU384	+	+	+	+	ASP258 (S1)	+	+	+	−
GLU411	−	−	+	−	CYS238 (S2)	−	−	−	+
HIS353	+	+	+	+	LYS240 (S2)	+	+	+	−
HIS383	+	+	+	+	GLY237 (S3)	−	−	−	+
HIS513	+	+	+	+	ILE249 (S4)	+	+	+	−
LYS511	−	+	+	+	**Colipase interacting residues**				
TYR523	+	+	+	+	ASP12	−	−	−	+
VAL380	+	−	+	+	GLN239	−	−	−	+
ZINC (II)	−	+	−	+	GLU13	−	−	−	+
					GLU15	−	−	−	+

+ or − symbols indicate presence or absence of the interaction, respectively.

[1] (S1–S4): indicate the four pancreatic lipase lid conformational steps in which the residues participate during hydrolysis of triglycerides.

study where CSP–SGD had a high content of proline principally in the middle or penultimate position and with cationic amino acids (histidine, lysine, and arginine) at a foremost frequency in the middle and the N-terminus (Supplementary Materials Table 1S). It is a consensus that ACE contains three binding pockets (S_1, S_1', and S_2') involved in the hydrolysis of angiotensin-I, thereby degrading bradykinin and increasing

blood pressure (Caballero, 2020; Bernstein, et al., 2013). The positive control (captopril) was used as a reference to assess the molecular docking (Supplementary Materials Table 1S) holding interactions with active sites (S₁) and (S₂) interacting with residues PHE457 and PHE527 as shown in other studies (Hall, et al., 2020). CSP-SGD inhibited ACE by multiple bonds and hydrophobic interactions with residues ALA354, VAL379/380, GLU162, HIS353/383, at the active site (S₁), HIS353/513, and LYS511 at the active site (S₂′), and interaction with ZN(II) and reactive GLU384 in HEXXH zinc-binding motif (Table 1). The interaction with the S₂′ pocket (HIS-313, HIS-353, TYR523, ALA 354) was frequent in this study. Similar results were observed by Xu et al. (2021), where hydrolyzed peptides derived from soybean (including IY, WMY, YVVF and LVLL) showed ACE inhibitory activity by forming H-bonds with HIS353 and HIS513 in S2 active pocket of ACE. S₂′ residues are involved in orienting the amide nitrogen in the substrate to accept hydrogens produced from nucleophilic attack of water by GLU3, which scissile amide nitrogen in the substrate facilitating cleavage.

Even though some peptides derived from CSP-SGD hold interactions with the active site of ACE, the kinetic observations indicated a non-competitive type inhibition. We hypothesized that a higher participation of glutamine-rich peptides with zinc ions might account for the observed activities from CSP-SGD on ACE. Since ACE is a zinc dependent dipeptidyl carboxypeptidase (Ianzer et al., 2007), zinc ions are key in the function of ACE. Therefore, Zn (II) interaction could impart non-competitive inhibitor attributes. For example, Ni, et al. (2012) identified a hexapeptide (TPTQQS) that acted as a non-competitive inhibitor. They demonstrated how the interaction of glutamine could convey non-competitive characteristics to a peptide by forcing the zinc ion away

from the active site and potentially triggering an active site conformation change. Our study also determined the interaction of glutamine-containing peptides QTPHQ and ELHPQ with Zn (II) coordination and could explain the non-competitive inhibition observed during the enzyme kinetics analysis. Consequently, future studies could be directed to understand quantitatively the presence of glutamine motifs of expression in canary seed proteins, and their correlation with ACE inhibition.

3.5. Identification and molecular docking analysis of CSP-SGD with pancreatic lipase inhibition

Based on affinity binding scores determined by molecular docking, the following four peptide sequences (VPPR, LADR, LSPR, and TVGPR) were identified as having the potential inhibitory activity towards pancreatic lipase. Table 1 shows the four peptides had negative GRAVY scores (−0.9 to −0.6) indicating intermediate hydrophobicity and binding energies (Affinity Energy) of (−6.2 to −5.9 kJ/mol), and interacting mainly with 11 residues from the binding interaction interphase of the pancreatic lipase and colipase domains. The positive control (orlistat) was used as a reference for molecular docking holding interactions (Supplementary Materials Table 2S) with active site residues SER153, HIS152, and HIS264 as reported in previous studies (Kokotos, 2003; Martinez-Gonzalez, et al., 2017). These interactions were found mainly to be by hydrogen bonding, followed by salt bridges and hydrophobic bonding (Fig. 5). At the access date for this study, a database search of CSP-SGD using the BIOPEP-UWM online server (http://www.uwm.edu.pl/biochemia/index.php/en/biopep, accessed 5/18/2021),
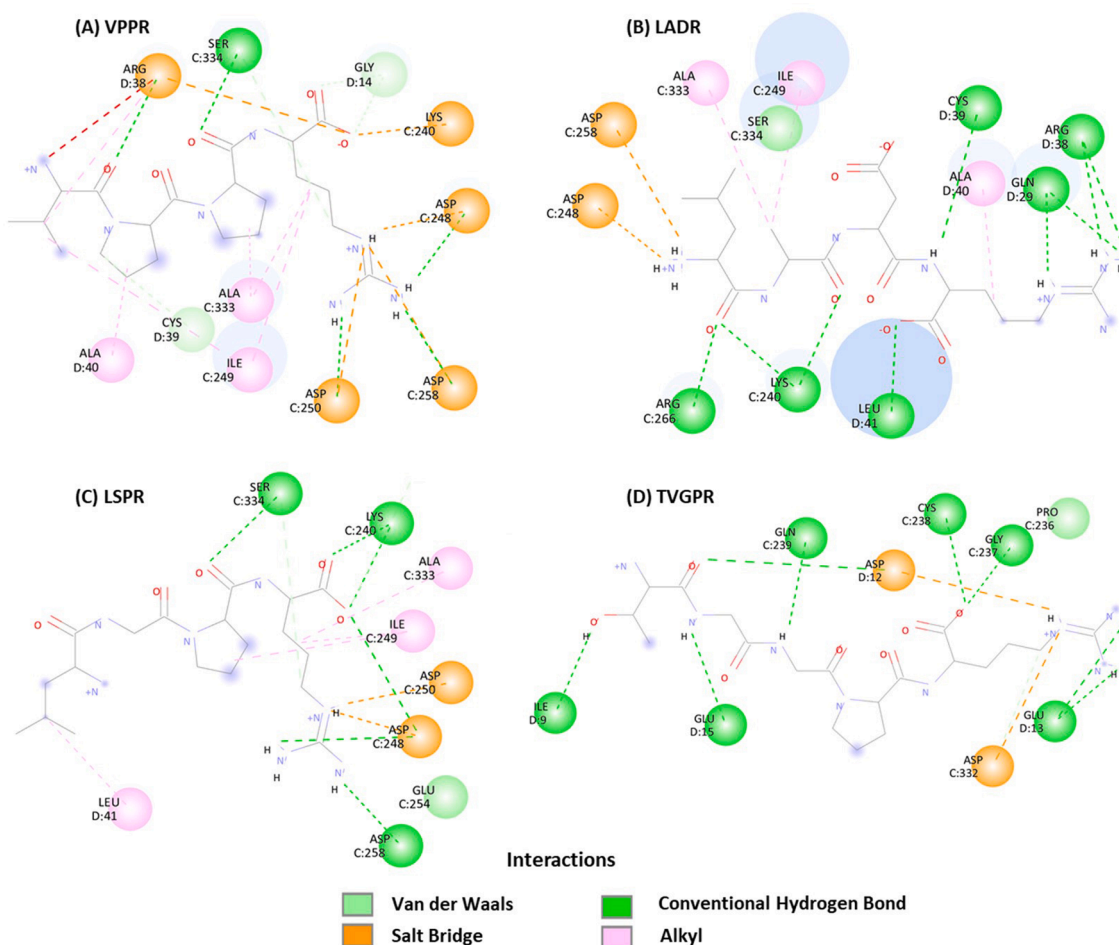

Fig. 5. Interaction of four canary seed peptide sequences (A-D) with the highest binding energy towards pancreatic lipase-colipase complex (1ETH).

showed no matches to any pancreatic lipase inhibitory peptides (Min-kiewicz, Iwaniak, & Darewicz, 2019). Some common validated pancreatic lipase inhibitory peptides identified in the search included: YGNPVGGVGH, RLARAGLAQ, LAPSTIK, and VAPEEHPV. Additionally, no structural motifs were identified between these peptides and the ones reported in this study. The limited information (only 18 antiobesity peptides have been reported in the database) and the insufficient data available on how peptides inhibit pancreatic lipase limits the database search and evidence the gap in research on the mechanisms of action of biopeptides against this enzyme. Nevertheless, studies on camel (*Camelus dromedarius*) milk (Mudgil et al., 2018), cocoa bean (*Theobroma cacao* L.) (Coronado-Cáceres et al., 2020), yellow field pea (*Pisum sativum* L.) (Awosika & Aluko, 2019), and pinto beans (*Phaseolus vulgaris*) (Ngoh, Choi, & Gan, 2017) provide insights on the understanding of the peptides' structural motifs and evidence the effect of non-polar residues to establish complex interactions with the lipophilic enzyme.

The molecular docking analysis revealed a higher rate of interaction of arginine with residues involved in keeping pancreatic lipase active. Although recent evidence shows that arginine-rich peptides might act as pancreatic lipase inhibitors (Stefanucci et al., 2019), their specific mechanism of action remains to be understood.

It is well recognized that pancreatic lipase largely contributes to the digestion of dietary fats, yielding small polar β–monoglycerides and fatty acids (Haque & Prabhu, 2016). During this process, pancreatic lipase activation occurs at the site where a 23-amino acid surface loop called "lid" (stretched from CYS238 and CYS262) is removed from the active site constituted by SER153, ASP177, and HIS264 in a four-step process (Haque & Prabhu, 2016). In this respect, ASP248, ASP250 and ASP258 residues are responsible for initiating lid movements during step 1 (S1) by coulombic forces, causing salt bridge bonds of ARG257 and ASP80 and H-bonds between ARG258 and TYR268 to be broken, helping to stabilize the open conformation of the lid (Haque & Prabhu, 2016). The four peptides could interfere with S1 interacting via hydrogen and salt bridges holding multiple bonds at a time with lipase and colipase residues (ASP248, ASP250, ASP258) (Table 1, Fig. 5). The interference of these peptides with CYS238 and LYS240 is associated with possible destabilization of disulfide bonds in step 2 (S2), where the separated lid is connected to the domain 1 (residues 1–336 of pancreatic lipase structure) via disulfide bonds with CYS238 (Table 1). On the other hand, peptide bonding to GLY237 and ILE249 may play an important role in steps 3 (S3) and 4 (S4), interfering with lid flexibility and reducing molecular mobility in the final step of the enzyme activation (Haque & Prabhu, 2016). Furthermore, peptides containing glycine interacted with GLU13 and GLU15 colipase's residues, and could block the lid conformation to return to its open state, thus preventing lipase from triggering further hydrolysis (Moreno-Córdova et al., 2020). The interference with the lid opening (S1-S4) and colipase corroborates the uncompetitive behavior observed in the kinetic analysis in this study (Fig. 2). Within the peptides that showed lipase inhibition, we identified that they had an exceptionally high content of hydrophobic amino acids (proline, leucine, and glycine) (Supplementary Materials Table 2S). More importantly arginine in the C-terminal of CSP-SGD showed to be the most relevant structural motif of inhibition (Fig. 5). In this context, we discovered that the frequency of interaction of hydrophobic amino acids from CSP-SGD with residues involved in stabilizing the active state of pancreatic lipase was 28%, lower than that observed for arginine alone (41%). This suggests that their primary role is to serve as stabilizing anchor points during enzyme-peptide interactions, where hydrophobic bonds are likely needed. Subsequently, exploring protein sources with high arginine content might be relevant in discovering novel lipase inhibitors.

4. Conclusions

In the present work, we determined that canary seed biopeptides produced with Alcalase remained stable after simulated gastrointestinal digestion (CSP-SGD), maintaining their bioactivity for ACE and DPP-IV, while enhancing it for pancreatic lipase. Kinetic analysis by Lineweaver-Burk plots revealed that CSP-SGD inhibit enzymes by mixed-type inhibition for DPP-IV and α-glucosidase; non-competitive inhibition for ACE; and uncompetitive inhibitor for pancreatic lipase. The peptide fractions, particularly fractions F5 and F7, also exhibited > 10% transport yield across the Caco-2 monolayer, suggesting that the peptides can have optimal transport through the epithelium.

For the first time, novel peptides sequences with potential antihypertensive (LHPQ, QTPHQ, KPVPR, and ELHPQ) and antiobesity (VPPR, LADR, LSPR, and TVGPR) activity were identified from canary seed protein. Molecular docking analysis revealed the importance of arginine, glycine, and hydrophobic amino acids in CSP-SGD, and their primary role in disrupting the proper function of the pancreatic lipase lid domain (CYS238-CYS262). Conversely, ACE inhibitory peptides were rich in proline, glutamine, and cationic residues, and could inhibit ACE by destabilization of the tetrahedral transition state, and zinc ions interaction leading to conformational changes. Taken together, these results suggest that canary seed peptides could serve as a promising therapeutic alternative and/or as functional, nutraceutical ingredients, even after gastrointestinal digestion. Future studies implementing peptide synthesis and molecular dynamics simulations will be valuable to validate the role of specific amino acids in the inhibition of enzymes such as ACE and pancreatic lipase. Finally, research should be geared towards understanding and assessing the health benefits and metabolic consequences of canary seed bioactive peptides *in vivo*.

Ethical statement

Hereby, I declare that all the data presented in the manuscript were produced by the Authors partnership and used with the permission of all the Authors.

CRediT authorship contribution statement

Uriel Urbizo-Reyes: Conceptualization, Methodology, Investigation, Data curation, Writing – original draft, Writing – review & editing. **Andrea M. Liceaga:** Conceptualization, Methodology, Data curation, Writing – review & editing, Supervision, Funding acquisition. **Lavanya Reddivari:** Conceptualization, Writing – review & editing. **Kee-Hong Kim:** Conceptualization, Writing – review & editing. **Joseph M. Anderson:** Conceptualization, Writing – review & editing.

Declaration of Competing Interest

The authors declare that they have no known competing financial interests or personal relationships that could have appeared to influence the work reported in this paper.

Funding

This work is supported by the USDA National Institute of Food and Agriculture, Hatch Act formula funds project 1019794.

Appendix A. Supplementary material

Supplementary data to this article can be found online at https://doi.org/10.1016/j.jff.2021.104892.

References

Aguilar-Toalá, J. E., & Liceaga, A. M. (2021). Cellular antioxidant effect of bioactive peptides and molecular mechanisms underlying: Beyond chemical properties. *International Journal of Food Science & Technology, 56*(5), 2193–2204.

Awosika, T. O., & Aluko, R. E. (2019). Inhibition of the in vitro activities of α-amylase, α-glucosidase and pancreatic lipase by yellow field pea (*Pisum sativum* L.) protein hydrolysates. *International Journal of Food Science & Technology, 54*(6), 2021–2034.

Bao, Z. J., Zhao, Y., Wang, X. Y., & Chi, Y. J. (2017). Effects of degree of hydrolysis (DH) on the functional properties of egg yolk hydrolysate with alcalase. *Journal of Food Science and Technology, 54*(3), 669–678.

Bhandari, D., Rafiq, S., Gat, Y., Gat, P., Waghmare, R., & Kumar, V. (2020). A review on bioactive peptides: Physiological functions, bioavailability and safety. *International Journal of Peptide Research and Therapeutics, 26*(1), 139–150.

Bernstein, K. E., Ong, F. S., Blackwell, W. L. B., Shah, K. H., Giani, J. F., Gonzalez-Villalobos, R. A., … Fuchs, S. (2013). A modern understanding of the traditional and nontraditional biological functions of angiotensin-converting enzyme. *Pharmacological Reviews, 65*(1), 1–46.

Bounouala, F. Z., Roudj, S., Karam, N.-E., Recio, I., & Miralles, B. (2017). Casein hydrolysates by Lactobacillus brevis and Lactococcus lactis proteases: Peptide profile discriminates strain-dependent enzyme specificity. *Journal of Agricultural and Food Chemistry, 65*(42), 9324–9332.

Caballero, J. (2020). Considerations for docking of selective angiotensin-converting enzyme inhibitors. *Molecules, 25*(2), 295.

CDC (Centers for Disease Control and Prevention). (2020). *Adult obesity facts*. Retrieved from: https://www.cdc.gov/obesity/data/adult.html.

Coronado-Cáceres, L. J., Rabadán-Chávez, G., Mojica, L., Hernández-Ledesma, B., Quevedo-Corona, L., & Lugo Cervantes, E. (2020). Cocoa seed proteins'(*Theobroma cacao* L.) anti-obesity potential through lipase inhibition using in silico, *In Vitro* and *In Vivo* models. *Foods, 9*(10), 1359.

Daskaya-Dikmen, C., Yucetepe, A., Karbancioglu-Guler, F., Daskaya, H., & Ozcelik, B. (2017). Angiotensin-I-converting enzyme (ACE)-inhibitory peptides from plants. *Nutrients, 9*(4), 316.

De Angelis, M., Siragusa, S., Vacca, M., Di Cagno, R., Cristofori, F., Schwarm, M., … Gobbetti, M. (2021). Selection of gut-resistant bacteria and construction of microbial consortia for improving gluten digestion under simulated gastrointestinal conditions. *Nutrients, 13*(3), 992.

Dueik, V., & Bouchon, P. (2016). Development of polyphenol-enriched vacuum and atmospheric fried matrices: Evaluation of quality parameters and *in vitro* bioavailability of polyphenols. *Food Research International, 88*, 166–172.

Estrada-Salas, P. A., Montero-Morán, G. M., Martínez-Cuevas, P. P., González, C., & Barba de la Rosa, A. P. (2014). Characterization of antidiabetic and antihypertensive properties of canary seed (*Phalaris canariensis* L.) peptides. *Journal of Agricultural and Food Chemistry, 62*(2), 427–433.

Hall, F., Johnson, P. E., & Liceaga, A. (2018). Effect of enzymatic hydrolysis on bioactive properties and allergenicity of cricket (*Gryllodes sigillatus*) protein. *Food Chemistry, 262*, 39–47. https://doi.org/10.1016/j.foodchem.2018.04.058

Hall, F., Reddivari, L., & Liceaga, A. M. (2020). Identification and characterization of edible cricket peptides on hypertensive and glycemic *In Vitro* inhibition and their anti-inflammatory activity on RAW 264.7 macrophage cells. *Nutrients, 12*(11), 3588.

Haque, N., & Prabhu, N. P. (2016). Lid closure dynamics of porcine pancreatic lipase in aqueous solution. *Biochimica et Biophysica Acta (BBA)-General Subjects, 1860*(10), 2313–2325.

Heitkamp, M., Siegrist, M., Molnos, S., Brandmaier, S., Wahl, S., Langhof, H., … Halle, M. (2021). Obesity genes and weight loss during lifestyle intervention in children with obesity. *JAMA Pediatrics, 175*(1), e205142.

Hermoso, J., Pignol, D., Kerfelec, B., Crenon, I., Chapus, C., & Fontecilla-Camps, J. C. (1996). Lipase activation by nonionic detergents: The crystal structure of the porcine lipase-colipase-tetraethylene glycol monooctyl ether complex. *Journal of Biological Chemistry, 271*(30), 18007–18016. https://doi.org/10.2210/pdb1ETH/pdb

Ianzer, D., Santos, R. A. S., Etelvino, G. M., Xavier, C. H., de Almeida Santos, J., Mendes, E. P., … de Camargo, A.n. C. M. (2007). Do the cardiovascular effects of angiotensin-converting enzyme (ACE) I involve ACE-independent mechanisms? New insights from proline-rich peptides of Bothrops jararaca. *Journal of Pharmacology and Experimental Therapeutics, 322*(2), 795–805.

Ibrahim, M. A., Bester, M. J., Neitz, A. W., & Gaspar, A. R. (2018). Structural properties of bioactive peptides with α-glucosidase inhibitory activity. *Chemical Biology & Drug Design, 91*(2), 370–379.

Karami, Z., & Akbari-Adergani, B. (2019). Bioactive food derived peptides: A review on correlation between structure of bioactive peptides and their functional properties. *Journal of food science and technology, 56*(2), 535–547.

Ketnawa, S., Suwal, S., Huang, J. Y., & Liceaga, A. M. (2018). Selective separation and characterisation of dual ACE and DPP-IV inhibitory peptides from rainbow trout (*Oncorhynchus mykiss*) protein hydrolysates. *International Journal of Food Science & Technology, 54*(4), 1062–1073.

Kokotos, G. (2003). Inhibition of digestive lipases by 2-oxo amide triacylglycerol analogues. *Journal of Molecular Catalysis B: Enzymatic, 22*(5–6), 255–269.

Kopp, W. (2019). How western diet and lifestyle drive the pandemic of obesity and civilization diseases. *Diabetes, Metabolic Syndrome and Obesity: Targets and Therapy, 12*, 2221.

Kumar, S., Narwal, S., Kumar, V., & Prakash, O. (2011). α-glucosidase inhibitors from plants: A natural approach to treat diabetes. *Pharmacognosy Reviews, 5*(9), 19.

Liu, W.-Y., Zhang, J.-T., Miyakawa, T., Li, G.-M., Gu, R.-Z., & Tanokura, M. (2021). Antioxidant properties and inhibition of angiotensin-converting enzyme by highly active peptides from wheat gluten. *Scientific Reports, 11*(1), 1–13.

Martinez-Gonzalez, A. I., Alvarez-Parrilla, E., Díaz-Sánchez, Á. G., de la Rosa, L. A., Núñez-Gastélum, J. A., Vazquez-Flores, A. A., & Gonzalez-Aguilar, G. A. (2017). In vitro inhibition of pancreatic lipase by polyphenols: A kinetic, fluorescence spectroscopy and molecular docking study. *Food Technology and Biotechnology, 55*(4), 519–530.

Mason, E., L'Hocine, L., Achouri, A., & Karboune, S. (2018). Hairless canaryseed: A novel cereal with health promoting potential. *Nutrients, 10*(9), 1327.

Mazloomi, S. N., Mora, L., Aristoy, M., Mahoonak, A. S., Ghorbani, M., Houshmand, G., & Toldrá, F. (2020). Impact of simulated gastrointestinal digestion on the biological activity of an alcalase hydrolysate of orange seed (*Siavaraze, Citrus sinensis*) by-products. *Foods, 9*(9), 1217.

Megías, C., Pedroche, J., del Mar Yust, M., Alaiz, M., Girón-Calle, J., Millán, F., & Vioque, J. (2009). Purification of angiotensin converting enzyme inhibitory peptides from sunflower protein hydrolysates by reverse-phase chromatography following affinity purification. *LWT-Food Science and Technology, 42*(1), 228–232.

Minekus, M., Alminger, M., Alvito, P., Ballance, S., Bohn, T., Bourlieu, C., et al. (2014). A standardised static in vitro digestion method suitable for food-an international consensus. *Food and Function, 5*(6), 1113–1124. https://doi.org/10.1039/C3FO60702J

Minkiewicz, P., Iwaniak, A., & Darewicz, M. (2019). BIOPEP-UWM database of bioactive peptides: Current opportunities. *International Journal of Molecular Sciences, 20*(23), 5978.

Montone, C. M., Capriotti, A. L., Cerrato, A., Antonelli, M., La Barbera, G., Piovesana, S., … Cavaliere, C. (2019). Identification of bioactive short peptides in cow milk by high-performance liquid chromatography on C18 and porous graphitic carbon coupled to high-resolution mass spectrometry. *Analytical and Bioanalytical Chemistry, 411*(15), 3395–3404.

Moreno-Córdova, E. N., Arvizu-Flores, A. A., Valenzuela-Soto, E. M., García-Orozco, K. D., Wall-Medrano, A., Alvarez-Parrilla, E., … González-Aguilar, G. A. (2020). Gallotannins are uncompetitive inhibitors of pancreatic lipase activity. *Biophysical Chemistry, 264*, Article 106409.

Mudgil, P., Kamal, H., Yuen, G. C., & Maqsood, S. (2018). Characterization and identification of novel antidiabetic and anti-obesity peptides from camel milk protein hydrolysates. *Food Chemistry, 259*, 46–54.

Natesh, R., Schwager, S. L., Sturrock, E. D., & Acharya, K. R. (2003). Crystal structure of the human angiotensin-converting enzyme–lisinopril complex. *Nature, 421*(6922), 551–554. https://doi.org/10.2210/pdb1O8A/pdb

Newstead, S. (2015). Molecular insights into proton coupled peptide transport in the PTR family of oligopeptide transporters. *Biochimica Et Biophysica Acta (BBA)-General Subjects, 1850*(3), 488–499.

Ngoh, Y.-Y., Choi, S. B., & Gan, C.-Y. (2017). The potential roles of Pinto bean (*Phaseolus vulgaris* cv. Pinto) bioactive peptides in regulating physiological functions: Protease activating, lipase inhibiting and bile acid binding activities. *Journal of Functional Foods, 33*, 67–75.

Ni, H., Li, L., Liu, G., & Hu, S.-Q. (2012). Inhibition mechanism and model of an angiotensin I-converting enzyme (ACE)-inhibitory hexapeptide from yeast (*Saccharomyces cerevisiae*). *PloS One, 7*(5), Article e37077.

Nongonierma, A. B., & FitzGerald, R. J. (2013). Dipeptidyl peptidase IV inhibitory properties of a whey protein hydrolysate: Influence of fractionation, stability to simulated gastrointestinal digestion and food–drug interaction. *International Dairy Journal, 32*(1), 33–39.

Nongonierma, A. B., Le Maux, S., Dubrulle, C., Barre, C., & FitzGerald, R. J. (2015). Quinoa (*Chenopodium quinoa* Willd.) protein hydrolysates with in vitro dipeptidyl peptidase IV (DPP-IV) inhibitory and antioxidant properties. *Journal of Cereal Science, 65*, 112–118.

Nuchprapha, A., Paisansak, S., Sangtanoo, P., Srimongkol, P., Saisavoey, T., Reamtong, O., … Karnchanatat, A. (2020). Two novel ACE inhibitory peptides isolated from longan seeds: Purification, inhibitory kinetics and mechanisms. *RSC Advances, 10*(22), 12711–12720.

Orio, L. P., Boschin, G., Recca, T., Morelli, C. F., Ragona, L., Francescato, P., … Speranza, G. (2017). New ACE-inhibitory peptides from hemp seed (*Cannabis sativa* L.) proteins. *Journal of Agricultural and Food Chemistry, 65*(48), 10482–10488.

Patterson, C. A., Malcolmson, L., Lukie, C., Young, G., Hucl, P., & Abdel-Aal, E. (2018). Glabrous canary seed: A novel food ingredient. *Cereal Foods World, 63*(5), 194–200.

Picariello, G., Iacomino, G., Mamone, G., Ferranti, P., Fierro, O., Gianfrani, C., … Addeo, F. (2013). Transport across Caco-2 monolayers of peptides arising from *in vitro* digestion of bovine milk proteins. *Food Chemistry, 139*(1–4), 203–212.

Ray, I., Mahata, S. K., & De, R. K. (2016). Obesity: An immunometabolic perspective. *Frontiers in Endocrinology, 7*, 157.

Ren, Y., Liang, K., Jin, Y., Zhang, M., Chen, Y., Wu, H., & Lai, F. (2016). Identification and characterization of two novel α-glucosidase inhibitory oligopeptides from hemp (*Cannabis sativa* L.) seed protein. *Journal of Functional Foods, 26*, 439–450.

Ring, B., Wrighton, S. A., & Mohutsky, M. (2014). Reversible mechanisms of enzyme inhibition and resulting clinical significance. *Enzyme Kinetics in Drug Metabolism, 37*–56.

Sánchez, A., & Vázquez, A. (2017). Bioactive peptides: A review. *Food Quality and Safety, 1*(1), 29–46. https://doi.org/10.1093/fqsafe/fyx006

Schwingshackl, L., Morze, J., & Hoffmann, G. (2020). Mediterranean diet and health status: Active ingredients and pharmacological mechanisms. *British Journal of Pharmacology, 177*(6), 1241–1257.

Song, H., Tian, Q., & Li, B. (2020). Novel Hyp-Gly-containing antiplatelet peptides from collagen hydrolysate after simulated gastrointestinal digestion and intestinal absorption. *Food & Function, 11*(6), 5553–5564.

Stefanucci, A., Luisi, G., Zengin, G., Macedonio, G., Dimmito, M. P., Novellino, E., & Mollica, A. (2019). Discovery of arginine-containing tripeptides as a new class of pancreatic lipase inhibitors. *Future Medicinal Chemistry, 11*(1), 5–19.

Sultana, R., Alashi, A. M., Islam, K., Saifullah, M., Haque, C. E., & Aluko, R. E. (2020). Inhibitory activities of polyphenolic extracts of Bangladeshi vegetables against α-amylase, α-glucosidase, pancreatic lipase, renin, and angiotensin-converting enzyme. *Foods, 9*(7), 844.

Trott, O., & Olson, A. J. (2010). AutoDock Vina: Improving the speed and accuracy of docking with a new scoring function, efficient optimization, and multithreading. *Journal of Computational Chemistry, 31*(2), 455–461.

Urbizo-Reyes, U., Aguilar-Toalá, J., & Liceaga, A. (2021). Hairless canary seeds (*Phalaris canariensis* L.) as a potential source of antioxidant, antihypertensive, antidiabetic, and antiobesity biopeptides. *Food Production, Processing and Nutrition, 3*(1), 1–12.

Urbizo-Reyes, U., San Martin-González, M. F., Garcia-Bravo, J., López Malo, A., & Liceaga, A. M. (2019). Physicochemical characteristics of chia seed (*Salvia hispanica*) protein hydrolysates produced using ultrasonication followed by microwave-assisted hydrolysis. *Food Hydrocolloids.* , Article 105187. https://doi.org/10.1016/j.foodhyd.2019.105187

Valverde, M. E., Orona-Tamayo, D., Nieto-Rendón, B., & Paredes-López, O. (2017). Antioxidant and antihypertensive potential of protein fractions from flour and milk substitutes from canary seeds (*Phalaris canariensis* L.). *Plant Foods for Human Nutrition, 72*(1), 20–25.

Vilcacundo, R., Martínez-Villaluenga, C., & Hernández-Ledesma, B. (2017). Release of dipeptidyl peptidase IV, α-amylase and α-glucosidase inhibitory peptides from quinoa (*Chenopodium quinoa* Willd.) during in vitro simulated gastrointestinal digestion. *Journal of Functional Foods, 35*, 531–539.

Wang, B., Xie, N., & Li, B. (2019). Influence of peptide characteristics on their stability, intestinal transport, and in vitro bioavailability: A review. *Journal of food biochemistry, 43*(1), Article e12571.

Wang, B., Yu, Z., Yokoyama, W., Chiou, B.-S., Chen, M., Liu, F., & Zhong, F. (2021). Collagen peptides with DPP-IV inhibitory activity from sheep skin and their stability to in vitro gastrointestinal digestion. *Food Bioscience*, Article 101161.

WHO. (2020a). Healthy diet. Retrieved from https://www.who.int/news-room/fact -sheets/detail/healthy-diet.

WHO. (2020b). Obesity. Retrieved from https://www.who.int/news-room/facts-in-pictu res/detail/6-facts-on-obesity.

Xie, N., Wang, B., Jiang, L., Liu, C., & Li, B. (2015). Hydrophobicity exerts different effects on bioavailability and stability of antioxidant peptide fractions from casein during simulated gastrointestinal digestion and Caco-2 cell absorption. *Food Research International, 76*, 518–526.

Xu, Q., Hong, H., Wu, J., & Yan, X. (2019). Bioavailability of bioactive peptides derived from food proteins across the intestinal epithelial membrane: A review. *Trends in Food Science & Technology, 86*, 399–411.

Xu, Z., Wu, C., Sun-Waterhouse, D., Zhao, T., Waterhouse, G. I., Zhao, M., & Su, G. (2021). Identification of post-digestion angiotensin-I converting enzyme (ACE) inhibitory peptides from soybean protein Isolate: Their production conditions and in silico molecular docking with ACE. *Food Chemistry, 345*, Article 128855.

Zhang, K., Sun, J., Fan, M., Qian, H., Ying, H., Li, Y., & Wang, L. (2021). Functional ingredients present in whole-grain foods as therapeutic tools to counteract obesity: Effects on brown and white adipose tissues. *Trends in Food Science & Technology*.

Zhu, Y.-T., Jia, Y.-W., Liu, Y.-M., Liang, J., Ding, L.-S., & Liao, X. (2014). Lipase ligands in Nelumbo nucifera leaves and study of their binding mechanism. *Journal of Agricultural and Food Chemistry, 62*(44), 10679–10686.